01 Jan 2006

Fast Time-Varying Dispersive Channel Estimation and Equalization for 8-PSK Cellular System

Sang-Yick Leong

Jingxian Wu

Chengshan Xiao
Missouri University of Science and Technology, xiaoc@mst.edu

Jan C. Olivier

Fast Time-Varying Dispersive Channel Estimation and Equalization for an 8-PSK Cellular System

Sang-Yick Leong, Jingxian Wu, Chengshan Xiao, *Senior Member, IEEE*, and Jan C. Olivier

***Abstract*—In this paper, a novel channel-estimation scheme for an 8-PSK enhanced data rates for GSM evolution (EDGE) system with fast time-varying and frequency-selective fading channels is presented. Via a mathematical derivation and simulation results, the channel impulse response (CIR) of the fast fading channel is modeled as a linear function of time during a radio burst in the EDGE system. Therefore, a least-squares-based method is proposed along with the modified burst structure for time-varying channel estimation. Given that the pilot-symbol blocks are located at the front and the end of the data block, the LS-based method is able to estimate the parameters of the time-varying CIR accurately using a linear interpolation. The proposed time-varying estimation algorithm does not cause an error floor that existed in the adaptive algorithms due to a nonideal channel tracking. Besides, the time-varying CIR in the EDGE system is not in its minimum-phase form, as is required for low-complexity reduced-state equalization methods. In order to maintain a good system performance, a Cholesky-decomposition method is introduced in front of the reduced-state equalizer to transform the time-varying CIR into its minimum-phase equivalent form. Via simulation results, it is shown that the proposed algorithm is very well suited for the time-varying channel estimation and equalization, and a good bit-error-rate performance is achieved even at high Doppler frequencies up to 300 Hz with a low complexity.**

***Index Terms*—Channel estimation, fast time-varying fading, frequency-selective fading.**

I. INTRODUCTION

ENHANCED data rates for GSM evolution (EDGE) was introduced to achieve higher data rates and spectral efficiency that is possible in current global system for mobile communications (GSM) and general packet radio service (GPRS) systems [1], [2]. In order to keep a backward compatibility with the second-generation cellular systems GSM and IS-136, the EDGE has a similar burst (slot) structure and system parameters as the GSM. Time-division multiple-access (TDMA) is used in the EDGE with a symbol period $T_s = 3.69\ \mu$s and a radio-burst length of 576.92 μs. Consequently, for static or slow-moving communication devices, it is reasonable to assume that the fading channel is time invariant during a burst. In general, this assumption is adopted in [3], [4], where various channel-estimation and equalization algorithms are developed or applied for the EDGE system with slow fading channels.

The application of the delayed decision-feedback sequence estimation (DDFSE) [5] and reduced-state sequence estimation (RSSE) [6] equalizers in the EDGE are discussed in [3], where the time-invariant channel was estimated with a least-squares (LS) method. In [4], a computationally efficient perturbation equalizer with a weighted LS channel estimation was proposed for the 8-PSK EDGE system, also assuming a time-invariant channel over the radio burst. The simulation results obtained in these references agree well with those obtained under ideal cases, i.e., a perfect channel estimation with a maximum likelihood sequence estimation (MLSE) equalizer.

For systems where subscribers travel at high speeds, a fast fading causes the channel impulse response (CIR) to vary significantly over the radio burst, i.e., it is a function of time. Therefore, the use of adaptive algorithms [3], [7]–[9], such as recursive-least-squares (RLS) and least-mean-squares (LMS) algorithms, are required in order to track the coefficients of the time-varying CIR over the radio burst. However, the adaptive RLS and/or LMS algorithms do not work very well under the time-varying channel in the EDGE system. This is mainly due to the delayed output of the MLSE equalizer and the use of the estimated symbols, which are causing an error propagation in updating the time-varying CIR. Reduced-state equalizers are essential in the EDGE, where an 8-PSK modulation is used due to complexity considerations. However, in the typical channel profiles of the EDGE system such as typical urban (TU) and hilly terrain (HT) profiles [2], the CIR of the frequency-selective fading channel is usually not in a minimum-phase form, i.e., the energy in the leading tap is very small compared to that of the second or third tap of the CIR. This may cause numerical instability problems when the reduced-state equalizers with a symbol feedback are utilized. Thus, in order to obtain a good performance with the use of the reduced-state equalization methods, a minimum-phase equivalent prefilter must be employed [3]. The finite-impulse response (FIR) prefilter can be obtained via a fast Cholesky factorization [10]–[13] or linear prediction (LP) [14]. In [3], Gerstacker and Schober employed the LMS algorithm to track the minimum-phase CIR of the time-varying channel. Alternatively, Chang and Georghiades proposed an iterative joint sequence and channel estimation for fast time-varying intersymbol interference (ISI) channels [15].

In this paper, an alternative to a channel tracking is proposed. A new method is introduced to eliminate the need for

Manuscript received November 18, 2003; revised March 31, 2005, October 20, 2005, and November 8, 2005. This work was supported in part by the National Science Foundation under Grant CCF-0514770 and the University of Missouri-Columbia Research Council under Grant URC-05-064. The review of this paper was coordinated by Prof. H. Leib.

S.-Y. Leong and C. Xiao are with the Department of Electrical and Computer Engineering, University of Missouri, Columbia, MO 65211 USA (e-mail: xiaoc@missouri.edu).

J. Wu is with the Department of Engineering Science, Sonoma State University, Rohnert Park, CA 94928 USA (e-mail: jingxian.wu@sonoma.edu).

J. C. Olivier is with the Department of Electrical Electronic Engineering, University of Pretoria, 0002 Pretoria, South Africa (e-mail: corne.olivier@eng.up.ac.za).

Digital Object Identifier 10.1109/TVT.2006.877465

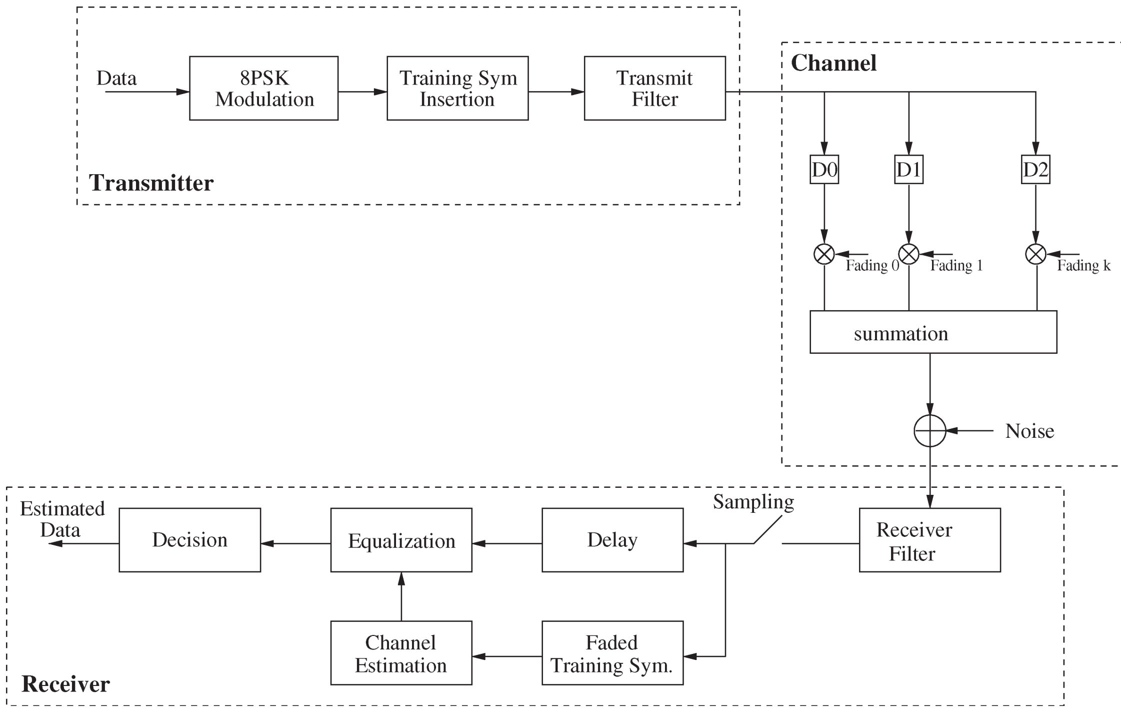

Fig. 1. Block diagram of the baseband EDGE system.

adaptive-tracking algorithms and the associated error floors. Initially, the burst format is slightly modified, but the pilot to data symbols ratio remains the same. This will be discussed in sections to follow. Second, it is shown that based on this modified burst, a linear interpolation of the CIR coefficients over time is used for most mobile speeds that occur in practice. A Cholesky-decomposition [12] step is then performed prior to the equalizer to transform the time-varying CIR over the entire burst to its minimum-phase equivalent form. Hence, the proposed algorithm requires no adaptive tracking of the CIR coefficients. The promising results demonstrate that the new method is able to perform well under the fast-fading conditions with the low complexity when compared to the adaptive-tracking algorithms. For systems where the mobile speed is slow, the performance is identical to the EDGE system, which assumes that the CIR is time invariant over the entire slot.

The rest of this paper is organized as follows. In Section II, the characteristics of the time-varying frequency-selective fading channel in the EDGE system are discussed, and a novel LS-based channel-estimation algorithm is proposed. Section III introduces the Cholesky-decomposition-based method to transform the estimated CIR to its minimum-phase form, and the obtained equivalent CIR is then used in the DDFSE or RSSE equalizers to detect the transmitted data. The computational complexity of the various estimation algorithms is presented in Section IV. Simulations are carried out in Section V to demonstrate the performance of the proposed algorithms, and Section VI concludes this paper.

II. Channel Estimation

In this section, the properties of the time-varying frequency-selective fading channels of the EDGE system are analyzed.

3	58	26	58	3	8.25
Tail	Data	Training Sequence	Data	Tail	Guard

(a)

3	13	58	58	13	3	8.25
Tail	Training Sequence	Data	Data	Training Sequence	Tail	Guard

(b)

Fig. 2. (a) Original EDGE slot structure. (b) Slightly modified slot structure.

Based on these properties, a channel-estimation algorithm, namely, the linear interpolated LS-based method is proposed.

A. Channel Characteristics

In Fig. 1, a block diagram of a baseband EDGE system is depicted. At the transmitter, the modulated 8-PSK symbols $x_k \in \{\exp[j(2\pi/8)q]; q = 0, 1, 2, \ldots, 7\}$ are placed in short burst, and a linearized Gaussian filter is used as the transmit filter. The original burst structure of the EDGE has 26 pilot symbols in the middle of each burst as shown in Fig. 2(a). This burst structure is good enough to be used for estimating the time-invariant channel state information of the entire burst. However, when the mobile subscriber is moving fast, the Doppler frequency is high, and the fading within one burst is no longer constant. Under these conditions, the original burst structure of the EDGE system cannot be used in estimating the time-varying CIR with a reasonable accuracy (see Section V). In what follows, an analysis of the channel characteristics in the EDGE system is performed, and it is shown that the CIR in a dispersive channel with a maximum Doppler frequency of 100 Hz may be modeled as a linear function of the time variable.

In this paper, the burst structure is slightly modified to facilitate the estimation of the time-varying fading channels in the 8-PSK system. In order to estimate the linear function accurately, it is proposed to split the 26 pilot symbols into two groups, placing the first group of 13 pilot symbols at the front of the data block and the second group of 13 symbols at the end of the data block. The modified burst structure is shown in Fig. 2(b). In the proposed modified burst structure, the data and training-symbols ratio still remains the same; hence, there is no loss in terms of the data rate achieved in the EDGE. Later, the simulation results show that there is no loss in the bit-error-rate (BER) performance, either if the fading is slow or the CIR remains constant, but the BER performance under the fast fading is significantly improved.

The modified burst structure is used throughout this paper. It is important to note here that the distance between the two blocks of the pilot symbols may affect the estimation of the linear function. Based on experimental results, the burst structure depicted in Fig. 2(b), which has a maximum separation between the two blocks of the pilot symbols achieves the best performance. In contrast, the original slot structure given in Fig. 2(a), which has no separation between the pilot symbols, therefore produces the worst results under the fast fading.

Assume that there is no timing error nor frequency offset at the receiver, then the baseband representation of the EDGE system shown in Fig. 1 can be written as

$$y_k = \sum_{l=0}^{L-1} h_k(l) x_{k-l} + n_k \tag{1}$$

where x_k is the transmitted 8-PSK symbol, y_k is the symbol rate sampled output of the receive filter, n_k is the additive white Gaussian noise (AWGN), and $h_k(l)$, $0 \le l \le L-1$, is the time-varying CIR of the fading channel. $h_k(l)$ is the symbol rate sampled version of the composite CIR that is the convolution of the transmit filter $P_T(\tau)$, the receive filter $P_R(\tau)$, and the physical CIR $g_c(t,\tau)$, which can be viewed as the response of the channel at time t to an impulse input at time $t-\tau$. The physical CIR has the form

$$g_c(t,\tau) = \sum_m \alpha_m(t) \delta(\tau - \tau_m) \tag{2}$$

where $\alpha_m(t)$ is the mth fading path with an average power $E[|\alpha_m(t)|^2]$ that is determined by the delay power profile of the channel, and τ_m is the delay of the mth fading path. In practical systems, the Doppler frequency is much smaller than the data rate, therefore, we can derive the equivalent discrete-time channel response $h_k(l)$ [16] as follows:

$$h_k(l) = h(kT_s, lT_s) \tag{3}$$

$$\begin{aligned} h(t,\tau) &= P_t(\tau) \otimes g_c(t,\tau) \otimes P_r(\tau) \\ &= \sum_m \alpha_m(t) R_{P_t P_r}(t - \tau_m) \end{aligned} \tag{4}$$

where $R_{P_t P_r}(t)$ is the correlation of the transmitting and receiving filters, and $\otimes$ is the convolution operator.

In the EDGE system, the linearized Gaussian filter and root-raised-cosine (RRC) filter are adopted as the transmit filter and receive filter, respectively. The linearized Gaussian filter [3], [17] is defined as follows:

$$c_0(t) = \begin{cases} \Pi_{j=0}^{3} s(t+jT), & 0 \le t \le 5T \\ 0, & \text{otherwise} \end{cases} \tag{5}$$

$$s(t) = \begin{cases} \sin\left(\pi \int_0^t g(\tau) d\tau\right), & 0 \le t < 4T \\ \sin\left(\frac{\pi}{2} - \pi \int_0^{(t-4T)} g(\tau) d\tau\right), & 4T \le t < 8T \\ 0, & \text{otherwise} \end{cases} \tag{6}$$

where $g(t)$ is the Gaussian-shaped frequency impulse of duration $4T$, and $T = 3.69\ \mu$s is the symbol duration of the EDGE system. The implementation of the linearized Gaussian filter will provide approximately identical transmit spectra between the EDGE and GSM systems [3], [18].

For the receive filter, we employ the RRC filter, which is a suboptimum filter [3], [19]. In [3], a numerical analysis for the influence of the suboptimum RRC filter on the BER performance is provided. It has been shown that the suboptimum RRC filter has only a small effect on the BER performance while compared to the optimum whitened matched filter. Due to the low complexity and near-optimum performance offered by the RRC filter, it is thus implemented as the receive filter in the EDGE system.

When the Doppler frequency f_d of the fading channel is in the range of [0, 20] Hz, the multipath fading channels can be considered as time invariant for one burst duration [3], [4], thus, the time variable k can be omitted in the representation of the CIR. Hence, the time-invariant CIR $h(l)$, $0 \le l \le L-1$ can be reliably estimated with the conventional LS-based methods. For typical fast fading channels, the CIR can no longer be treated as time invariant. It will be shown next that the fading channel can be approximated as a linear function of the time variable.

The mth path of the fading channel can be written as [20]

$$\alpha_m(t) = E_m \sum_{n=1}^{N} C_{nm} \exp\left[j(\omega_\mathrm{d} t \cos\beta_{nm} + \phi_{nm})\right] \tag{7}$$

where E_m is a scaling constant, $\omega_\mathrm{d} = 2\pi f_\mathrm{d}$, β_{nm}, and ϕ_{nm} are statistically independent random variables, and they are uniformly distributed on $[-\pi, \pi)$. After some algebraic manipulations, we can get

$$\alpha_m(t) = \alpha_{cm}(t) + j\alpha_{sm}(t) \tag{8}$$

$$\begin{aligned} \alpha_{cm}(t) = E_m \sum_{n=1}^{N} C_{nm} \{&\cos(\omega_\mathrm{d} t \cos\beta_{nm}) \cos\phi_{nm} \\ &- \sin(\omega_\mathrm{d} t \cos\beta_{nm}) \sin\phi_{nm}\} \end{aligned} \tag{9}$$

$$\begin{aligned} \alpha_{sm}(t) = E_m \sum_{n=1}^{N} C_{nm} \{&\sin(\omega_\mathrm{d} t \cos\beta_{nm}) \cos\phi_{nm} \\ &+ \cos(\omega_\mathrm{d} t \cos\beta_{nm}) \sin\phi_{nm}\}. \end{aligned} \tag{10}$$

While $f_\mathrm{d} \le 100$ Hz, $|\omega_\mathrm{d} t \cos(\beta_{nm})| \le 0.3625$ radians for $0 \le t \le 576.92\ \mu$. As a result, the following approximations

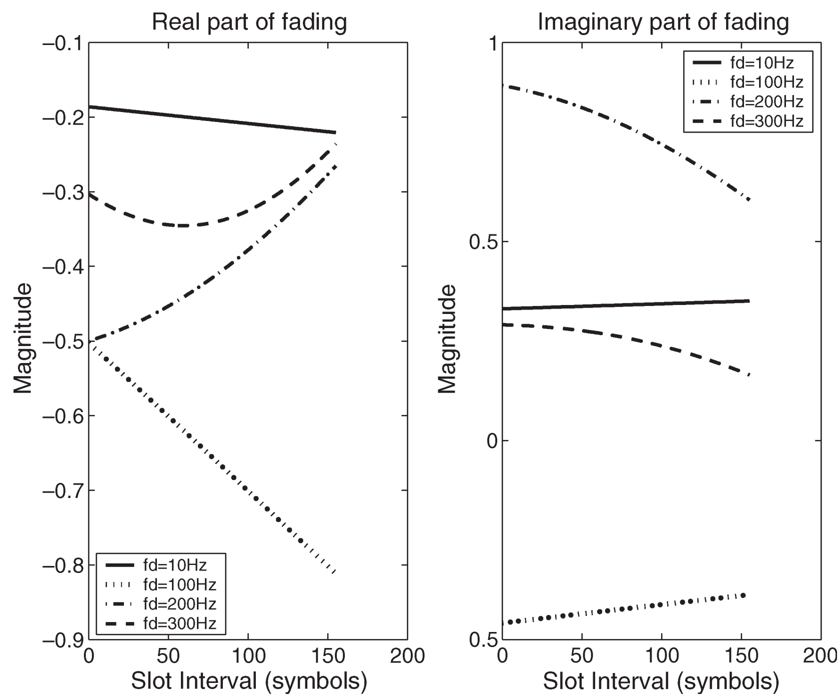

Fig. 3. Real and imaginary part of the Rayleigh fading in one slot interval at $f_\mathrm{d} = 10, 100, 200,$ and 300 Hz.

are valid by an implementation of the small angle rule $\cos x \approx 1$ and $\sin x \approx x$:

$$\tilde{\alpha}_{cm}(t) = E_m \sum_{n=1}^{N} C_{nm}\{\cos\phi_{nm} - t\omega_\mathrm{d}\cos\beta_{nm}\sin\phi_{nm}\} \quad (11)$$

$$\tilde{\alpha}_{sm}(t) = E_m \sum_{n=1}^{N} C_{nm}\{\sin\phi_{nm} + t\omega_\mathrm{d}\cos\beta_{nm}\cos\phi_{nm}\}. \quad (12)$$

It is apparent that $\alpha_m(t)$ can be approximated as a linear function of the time variable t, and so can $h_k(l)$, which is a linear function of $\alpha_m(t)$, as long as f_d (Doppler frequency) is less or equal to 100 Hz. This analysis is supported by Fig. 3, which clearly shows the real and imaginary parts of one tap of a typical CIR within one burst duration with Doppler frequency $f_\mathrm{d} = 10, 100, 200,$ and 300 Hz.

Now, consider a Doppler frequency up to 300 Hz. It is clear that the CIR is not necessary as a linear or constant from the analysis above. According to [20], β_{nm} is assumed to be uniformly distributed on $[-\pi, \pi)$. Therefore, there are some cases where the fading-channel taps may exhibit a parabolic/oscillatory behavior with a minimum or maximum peak. As a consequence, the BER performance will be degraded under these conditions. In Section V, the simulation results indicate that the new method can combat the Doppler frequency effectively up to 300 Hz, even though the parabolic behavior can exist.

B. Channel Estimation

Having analyzed the characteristics of the Rayleigh fading channel, we consider now the estimation of the time-varying frequency-selective CIR $h_k(l)$.

Based on the analysis in Section II-A, it is proposed to approximate the CIR $h_k(l)$ as a linear function of the time variable k,

$$h_k(l) = u_0(l) + k u_1(l) \quad (13)$$

where $u_0(l)$ and $u_1(l)$ are parameters to be estimated. For a time-varying frequency-selective fading channel with a channel length L, there are $2L$ parameters to be estimated for each burst, and the CIR of one burst can be linearly approximated by these parameters.

From (1) and (13), the kth received sample y_k can be represented as

$$y_k = \mathbf{x}_k(\mathbf{u}_0 + k \cdot \mathbf{u}_1) + n_k \quad (14)$$

where $\mathbf{x}_k = [x_k, x_{k-1}, \ldots, x_{k-L+1}] \in \mathbb{C}^{1\times L}$ are the transmitted symbols, and $\mathbf{u}_j = [u_j(0), u_j(1), \ldots, u_j(L-1)]^\mathrm{T} \in \mathbb{C}^{L\times 1}$, for $j = 0$, 1, with $(\cdot)^\mathrm{T}$ representing the transpose. With the known training symbols transmitted at the beginning and the end of each burst, the received samples contributed by the training symbols can be written into a matrix format

$$\boldsymbol{y} = \mathbf{A}\cdot\mathbf{u}_0 + \mathbf{T}\cdot\mathbf{A}\cdot\mathbf{u}_1 + \boldsymbol{n} \quad (15)$$

$$= [\,\mathbf{A} \quad \mathbf{T}\cdot\mathbf{A}\,]\begin{bmatrix}\mathbf{u}_0\\ \mathbf{u}_1\end{bmatrix} + \boldsymbol{n} \quad (16)$$

where

$$\boldsymbol{y} = [\,y_{L-1} \quad \cdots \quad y_{15} \quad y_{132+L-1} \quad \cdots \quad y_{147}\,]^\mathrm{T} \in \mathbb{C}^{(34-2L)\times 1} \quad (17)$$

$$\boldsymbol{n} = [\,n_{L-1} \quad \cdots \quad n_{15} \quad n_{132+L-1} \quad \cdots \quad n_{147}\,]^\mathrm{T} \in \mathbb{C}^{(34-2L)\times 1} \quad (18)$$

$$\mathbf{A} = \begin{bmatrix} x_{L-1} & x_{L-2} & \cdots & x_1 & x_0 \\ \vdots & & \vdots & & \vdots \\ x_{15} & x_{14} & \cdots & x_{15-L+2} & x_{15-L+1} \\ x_{132+L-1} & x_{132+L-2} & \cdots & x_{133} & x_{132} \\ \vdots & & \vdots & & \vdots \\ x_{147} & x_{146} & \vdots & x_{147-L+2} & x_{147-L+1} \end{bmatrix} \in \mathbb{C}^{(34-2L)\times L} \tag{19}$$

and $\mathbf{T}$ is a diagonal matrix defined as

$$\mathbf{T} = \mathrm{diag}\{L-1, \ldots, 14, 15, 132+L-1, \ldots, 146, 147\}. \tag{20}$$

With (16), the cost function for an LS criterion can be defined as follows:

$$J_{\mathrm{LS}} = (\boldsymbol{y} - \Phi\mathbf{u})^{\mathrm{H}}(\boldsymbol{y} - \Phi\mathbf{u}) \tag{21}$$

where $\Phi = [\mathbf{A}\ \mathbf{TA}]$, $\mathbf{u} = [\mathbf{u}_0^{\mathrm{T}}\ \mathbf{u}_1^{\mathrm{T}}]^{\mathrm{T}}$ and $(\cdot)^{\mathrm{H}}$ is the Hermitian transpose operator. The $\hat{\mathbf{u}}$ that minimizes J_{LS} can be obtained from the equation $\partial J_{\mathrm{LS}}/\partial \mathbf{u}^{\mathrm{H}} = 0$, and the solution is

$$\hat{\mathbf{u}} = \underbrace{\begin{bmatrix} \mathbf{A}^{\mathrm{H}}\mathbf{A} & \mathbf{A}^{\mathrm{H}}\mathbf{TA} \\ \mathbf{A}^{\mathrm{H}}\mathbf{TA} & \mathbf{A}^{\mathrm{H}}\mathbf{T}^2\mathbf{A} \end{bmatrix}^{-1}}_{\boldsymbol{\Psi}^{-1}} \begin{bmatrix} \mathbf{A}^{\mathrm{H}}\boldsymbol{y} \\ \mathbf{A}^{\mathrm{H}}\mathbf{T}\boldsymbol{y} \end{bmatrix} \tag{22}$$

where $\Psi = \Phi^{\mathrm{H}}\Phi$. In what follows, a recursive procedure is outlined for the computation of $\hat{\mathbf{u}}$. This will actually eliminate the computation of the matrix inversion Ψ^{-1} in (22). Denote $\boldsymbol{y}_i$ as the ith component of the column vector $\boldsymbol{y}$. Similarly, define $\boldsymbol{n}_i$. Based on the (16)–(19), the ith received sample of $\boldsymbol{y}$ is expressed by

$$\boldsymbol{y}_i = \Phi_i\mathbf{u} + \boldsymbol{n}_i \quad \text{for } i = 1, 2, \ldots, (34-2L) \tag{23}$$

where $\Phi_i \in \mathbb{C}^{1\times 2L}$ is the ith row of the matrix Φ. From (23), the estimated $\hat{\mathbf{u}}$ at index i, namely $\hat{\mathbf{u}}(i)$ can be found by using the approach of minimizing the residual sum of squares defined by $J(i) = \sum_{j=1}^{i}[\boldsymbol{y}_j - \Phi_j\mathbf{u}]^\star[\boldsymbol{y}_j - \Phi_j\mathbf{u}]$ [7], [21], and $(\cdot)^\star$ is the complex conjugate. Thus, the estimated $\hat{\mathbf{u}}(i)$ is derived as

$$\hat{\mathbf{u}}(i) = \underbrace{\left[\sum_{j=1}^{i}\Phi_j^{\mathrm{H}}\Phi_j\right]^{-1}}_{\boldsymbol{\Psi}^{-1}(i)} \left[\sum_{j=1}^{i}\Phi_j^{\mathrm{H}}\boldsymbol{y}_j\right] \tag{24}$$

where $\Psi(i) = \sum_{j=1}^{i}\Phi_j^{\mathrm{H}}\boldsymbol{\Phi}_j \in \mathbb{C}^{2L\times 2L}$ is a nonnegative definite correlation matrix. In order to ensure that the correlation matrix $\Psi(i)$ is always positive definite, and therefore nonsingular, we define $\Psi(0) = c\mathbf{I}$ where c is a small positive constant and $\mathbf{I} \in \mathbb{C}^{2L\times 2L}$ is the identity matrix; thus, each element on the main diagonal of correlation matrix $\Psi(i)$ is added to a small positive constant c [21]. Now, using the matrix-inversion lemma, the inverse of matrix $\Psi(i)$ can be computed recursively by

$$\Psi(i) = \Phi_i^{\mathrm{H}}\Phi_i + \Psi(i-1) \tag{25}$$

$$\begin{aligned}\Psi^{-1}(i) &= \Psi^{-1}(i-1) - \frac{\Psi^{-1}(i-1)\Phi_i^{\mathrm{H}}}{1 + \Phi_i\Psi^{-1}(i-1)\Phi_i^{\mathrm{H}}}\Phi_i\Psi^{-1}(i-1) \\ &= \Psi^{-1}(i-1) - \boldsymbol{\kappa}(i)\Phi_i\Psi^{-1}(i-1)\end{aligned} \tag{26}$$

where $\boldsymbol{\kappa}(i) = ((\Psi^{-1}(i-1)\Phi_i^{\mathrm{H}})/\ (1 + \Phi_i\Psi^{-1}(i-1)\Phi_i^{\mathrm{H}})) \in \mathbb{C}^{2L\times 1}$ is the gain vector. According to the derivation steps given in [21, pp.566–577], the gain vector $\boldsymbol{\kappa}(i)$ equals to $\Psi(i)^{-1}\Phi_i^{\mathrm{H}}$. At last, using (26) and $\boldsymbol{\kappa}(i)$, the estimated $\hat{\mathbf{u}}(i)$ in (24) can be written as follows:

$$\begin{aligned}\hat{\mathbf{u}}(i) &= \left[\Psi^{-1}(i-1) - \boldsymbol{\kappa}(i)\Phi_i\Psi^{-1}(i-1)\right] \\ &\quad \times \left[\sum_{j=1}^{i-1}\Phi_j^{\mathrm{H}}\boldsymbol{y}_j + \Phi_i^{\mathrm{H}}\boldsymbol{y}_i\right] \\ &= \Psi^{-1}(i-1)\sum_{j=1}^{i-1}\Phi_j^{\mathrm{H}}\boldsymbol{y}_j + \boldsymbol{\kappa}(i) \\ &\quad \times \left[\boldsymbol{y}_i - \Phi_i\left(\Psi^{-1}(i-1)\sum_{j=1}^{i-1}\Phi_j^{\mathrm{H}}\boldsymbol{y}_j\right)\right] \\ &= \hat{\mathbf{u}}(i-1) + \boldsymbol{\kappa}(i)[\boldsymbol{y}_i - \Phi_i\hat{\mathbf{u}}(i-1)].\end{aligned} \tag{27}$$

Thus, it is found that the inversion of the correlation matrix Ψ^{-1} in (22) is now replaced by the inversion of scalar $\{1 + \Phi_i\Psi^{-1}(i-1)\Phi_i^{\mathrm{H}}\}$ in estimating $\mathbf{u}$.

With the estimation of the parameters $\mathbf{u}_0$ and $\mathbf{u}_1$, the CIR of the entire burst can be easily obtained from (13). It is important to note that when Ψ is deterministic, and the noise is zero-mean white Gaussian noise, the LS-based algorithm estimator, (22) and (27), is a linear unbiased estimator. The CIR information is then used in the equalizer to recover the original transmitted data.

III. Channel Equalization

For an 8-PSK constellation in the frequency-selective fading channel, where the channel length $L > 4$, the use of the MLSE with the Viterbi Algorithm (VA) as the equalizer is impractical due to an excessive computational complexity. It is shown in [3] that the DDFSE and RSSE algorithms are promising equalization techniques for the EDGE system. However, these algorithms can only be applied to systems with a minimum-phase CIR, otherwise, a performance degradation will occur. For a system with a time-invariant CIR, a prefilter can be used to obtain an equivalent CIR with the minimum phase [3], [22], but the prefilter approach is not applicable to systems with time-varying CIR without resorting to a channel tracking. Additionally, there is also a performance loss due to the nonideal channel tracking in the time-varying channel [3], [23]. In this section, a Cholesky-decomposition-based method is introduced to obtain the equivalent minimum-phase CIR for the time-varying fading channels without resorting to the channel tracking.

For the purpose of simplicity, here, the first and second data blocks of one burst are defined together, i.e., $\underline{\mathbf{y}} = [y_{16}, y_{17}, \ldots, y_{131}]^{\mathrm{T}} \in \mathbb{C}^{N_{\mathrm{d}}\times 1}$, where $N_{\mathrm{d}} = 116$ is the length of the entire data block. Based on the estimated time-varying CIR $\hat{H}_k(l)$ and (1), the input–output relationship of the data block can be written into a matrix format, shown in (28) at the bottom of the page, or in a compact form as

$$\underline{\mathbf{y}} = \underline{\mathbf{H}} \cdot \underline{\mathbf{x}} + \underline{\mathbf{n}}. \tag{29}$$

For typical channel profiles, such as the TU profile and HT profile [2], the impulse responses of the frequency-selective fading channels are usually not in the minimum-phase forms, i.e., the energy of $h_k(1)$ and $h_k(2)$ is significantly larger than that of $h_k(0)$. Hence, the CIR matrix $\underline{\mathbf{H}} \in \mathbb{C}^{N_{\mathrm{d}}\times(N_{\mathrm{d}}+L-1)}$ formed with this CIR is not diagonally dominant, which may cause numerical instability problems when the DDFSE or RSSE equalizers with feedback are used.

The objective here is to find an equivalent system with the minimum-phase CIR, whose input–output relationship of the equivalent system can be represented as

$$\mathbf{W}\underline{y} = \mathbf{B}\underline{\mathbf{x}} + \underline{\boldsymbol{e}} \tag{30}$$

where $\mathbf{W} \in \mathbb{C}^{(N_{\mathrm{d}}+L-1)\times N_{\mathrm{d}}}$, $\mathbf{B} \in \mathbb{C}^{(N_{\mathrm{d}}+L-1)\times(N_{\mathrm{d}}+L-1)}$, and $\underline{\boldsymbol{e}} \in \mathbb{C}^{(N_{\mathrm{d}}+L-1)\times 1}$ are the feed forward matrix, CIR feedback matrix, and the noise vector of the equivalent system, respectively [12], [24]. In order to effectively equalize the time-varying frequency-selective fading channel using the reduced-state equalizers, the CIR matrix $\mathbf{B}$ should satisfy the following two conditions: 1) $\mathbf{B}$ should minimize the variance of the noise component of the system; 2) $\mathbf{B}$ should be a lower triangular matrix with most of the time-varying CIR energy concentrated in the first few taps. The first condition will improve the performance of the equalizer, and the second condition can guarantee a system with the minimum-phase CIR. Therefore, the same approach as the minimum mean-squared-error (MMSE)-decision-feedback equalizer (DFE) algorithm introduced by Al-Dhahir and Cioffi [12] is implemented here to achieve this goal.

The variance of the noise component of the equivalent system is

$$\sigma_e^2 = \frac{1}{N_{\mathrm{d}}}\mathrm{trace}\left\{E\left[(\mathbf{B}\underline{\mathbf{x}} - \mathbf{W}\underline{y})(\mathbf{B}\underline{\mathbf{x}} - \mathbf{W}\underline{y})^{\mathrm{H}}\right]\right\} \tag{31}$$

TABLE I
SUMMARY OF THE PROPOSED CHANNEL-ESTIMATION AND EQUALIZATION ALGORITHMS

1. Perform channel estimation by recursive algorithm:
Define $\Psi(0) = c\mathbf{I}$ and $\hat{\mathbf{u}}(0) = 0$
Loop from j=1 to i
Compute gain vector $\kappa(i)$
Update $\hat{\mathbf{u}}(i)$:
$\hat{\mathbf{u}}(i) = \hat{\mathbf{u}}(i-1) + \kappa(i)[\mathbf{y}_i - \Phi_i\hat{\mathbf{u}}(i-1)]$
End of loop
2. Generate the approximate CIR $h_k(l)$:
$h_k(l) = u_0(l) + ku_1(l)$
3. Calculate lower triangular matrix $\mathbf{U}$:
$\mathbf{U}^h\mathbf{U} = \frac{1}{\mathrm{SNR}}\mathbf{I}_{N_d+L-1} + \underline{\mathbf{H}}^H\underline{\mathbf{H}}$
4. Apply reduced state equalizers for channel equalization:
$(\mathbf{U}^H)^{-1}\underline{\mathbf{H}}^H\underline{\mathbf{y}} = \mathbf{U}\underline{\mathbf{x}} + \underline{\mathbf{e}}$

where trace$(\cdot)$ will return the sum of the diagonal elements of a matrix. According to the orthogonality principle [19, pp.256–258], the matrix $\mathbf{B}$ minimizing σ_e^2 must satisfy $\mathbf{B} \cdot \mathbf{R}_{xy} = \mathbf{W} \cdot \mathbf{R}_{yy}$, where $\mathbf{R}_{AB} = E(\underline{\mathbf{A}} \cdot \underline{\mathbf{B}}^{\mathrm{H}})$. Therefore, the minimum value of σ_e^2 can be obtained as

$$\min(\sigma_e^2) = \frac{1}{N_{\mathrm{d}}}\mathrm{trace}\left[\mathbf{B}\left(\mathbf{R}_{xx} - \mathbf{R}_{xy}\mathbf{R}_{yy}^{-1}\mathbf{R}_{yx}\right)\mathbf{B}^{\mathrm{H}}\right] \tag{32}$$

$$= \frac{\sigma_n^2}{N_{\mathrm{d}}} \cdot \mathrm{trace}\left[\mathbf{B}\left(\frac{1}{\mathrm{SNR}}\mathbf{I}_{N_{\mathrm{d}}+L-1} + \underline{\mathbf{H}}^{\mathrm{H}}\underline{\mathbf{H}}\right)^{-1}\mathbf{B}^{\mathrm{H}}\right] \tag{33}$$

$$= \frac{\sigma_n^2}{N_{\mathrm{d}}} \cdot \mathrm{trace}\left[\mathbf{B}\mathbf{U}^{-1}(\mathbf{U}^{\mathrm{H}})^{-1}\mathbf{B}^{\mathrm{H}}\right] \tag{34}$$

where $\mathbf{U} \in \mathbb{C}^{(N_{\mathrm{d}}+L-1)\times(N_{\mathrm{d}}+L-1)}$ is a lower triangular matrix from the Cholesky decomposition. The expression (33) is based on the assumption that the input data symbols x_k are independent, i.e., $\mathbf{R}_{xx} = E_s\mathbf{I}_{N_{\mathrm{d}}+L-1}$ with E_s being the symbol energy, and σ_n^2 is the variance of the AWGN n_k, while the signal-to-noise ratio $\mathrm{SNR} = E_s/\sigma_n^2$.

$$\begin{bmatrix} y_{16} \\ y_{17} \\ \vdots \\ y_{130} \\ y_{131} \end{bmatrix} = \begin{bmatrix} \hat{h}_{16}(L-1) & \cdots & \hat{h}_{16}(1) & \hat{h}_{16}(0) & 0 & \cdots & \cdots & 0 \\ 0 & \hat{h}_{17}(L-1) & \cdots & \hat{h}_{17}(1) & \hat{h}_{17}(0) & 0 & \cdots & \cdots \\ \vdots & 0 & \ddots & \ddots & \ddots & \ddots & 0 & \cdots \\ 0 & \cdots & 0 & \hat{h}_{130}(L-1) & \cdots & \hat{h}_{130}(1) & \hat{h}_{130}(0) & 0 \\ 0 & \cdots & \cdots & 0 & \hat{h}_{131}(L-1) & \cdots & \hat{h}_{131}(1) & \hat{h}_{131}(0) \end{bmatrix} \times \begin{bmatrix} x_{16-L+1} \\ x_{16-L+2} \\ \vdots \\ x_{130} \\ x_{131} \end{bmatrix} + \begin{bmatrix} n_{16} \\ n_{17} \\ \vdots \\ n_{130} \\ n_{131} \end{bmatrix} \tag{28}$$

TABLE II
NUMBER OF REQUIRED OPERATIONS PER PILOT AND DATA SYMBOL USING VARYING CHANNEL-ESTIMATION ALGORITHMS, WHERE L IS THE CIR LENGTH

		Complexity		
		LS	New Method	RLS
Pilot symbol	real multiplications	$6L^2+3L$	$4(6L^2+3L)-6L$	$6L^2+3L$
	real additions	$5L^2$	$4(5L^2)$	$5L^2$
Data symbol	real multiplications	0	L	$6L^2+3L$
	real additions	0	L	$5L^2$

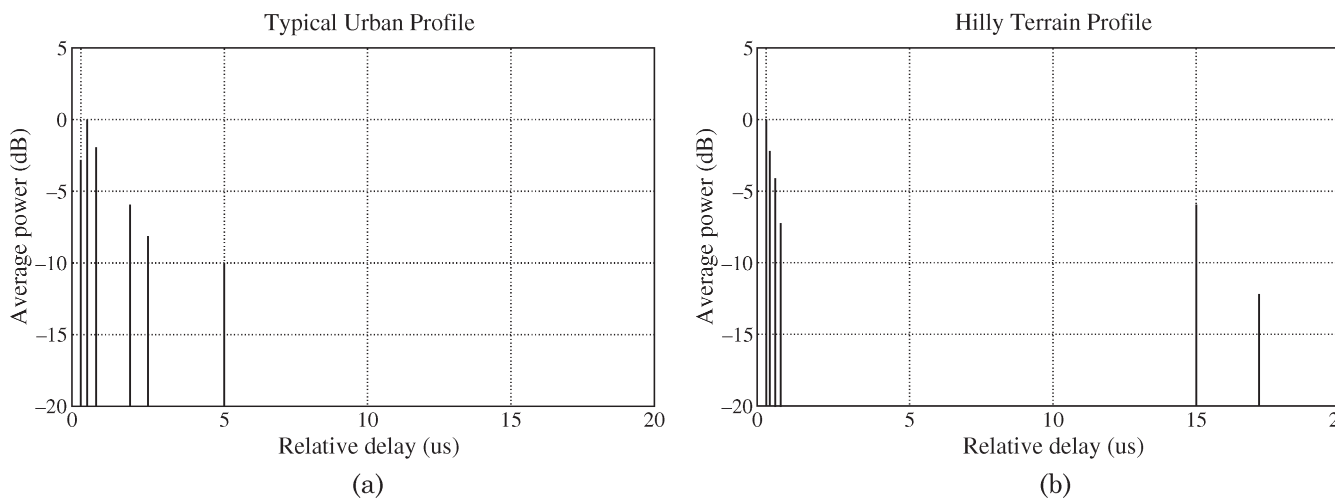

Fig. 4. Typical channel profiles of the EDGE system. (a) TU propagation model and (b) HT propagation model.

Therefore, the equivalent CIR matrix $\mathbf{B}$ is

$$\mathbf{B} = \mathbf{U} \tag{35}$$

$$\mathbf{W} = (\mathbf{U}^{\mathrm{H}})^{-1}\underline{\mathbf{H}}^{\mathrm{H}}. \tag{36}$$

From the above equations, the input–output relationship of the equivalent system can be written as

$$(\mathbf{U}^{\mathrm{H}})^{-1}\underline{\mathbf{H}}^{\mathrm{H}}\underline{\mathbf{y}} = \mathbf{U}\underline{\mathbf{x}} + \underline{e} \tag{37}$$

where the matrix $\mathbf{U}$ has a time-varying CIR energy concentrated in the first few taps. The obtained equivalent CIR matrix can then be used in the DDFSE or RSSE equalizer to estimate the original transmitted symbols. In what follows, we summarize the proposed channel-estimation and equalization algorithm in Table I.

It is important to note that the concept of Cholesky decomposition introduced in this paper demonstrates that it is possible to transform the time-varying CIR into its minimum-phase equivalent form. For efficient computational algorithms, the fast Cholesky factorization is proposed in papers [10]–[13], and the details are thus omitted here.

IV. COMPUTATIONAL COMPLEXITY

An important aspect of the channel-estimation algorithms is their computational complexity. In this paper, the LS algorithm (without channel tracking) given in [3], the proposed linear interpolated LS-based method, and the adaptive RLS algorithm [21] are considered for comparison.

Table II shows the required number of real multiplications and additions per pilot, and data symbols to estimate the CIR. The recursive procedures implemented in the estimation algorithms above are to avoid the matrix inversion. All of the algorithms employ the LS estimator, while the pilot-symbol blocks are used to estimate the parameters of the CIR. The LS and RLS require $6L^2 + 3L$ real multiplications and $5L^2$ real additions per pilot symbol, and the new method requires about four times as much as that of the LS algorithm. To track the time-varying channel using the data symbols, the LS method requires 0 steps, since the CIR is assumed constant for the entire burst. The RLS algorithm requires the same number of computation operations as for the pilot symbols. However, the proposed method in this paper requires only L real multiplications and L real additions in updating the CIR for the data symbols. In the next section, it is shown that the proposed method, which is using only a small number of operations, can effectively combat the Doppler frequency up to 300 Hz.

V. SIMULATION RESULTS

In this section, simulations are carried out to evaluate the performance of the proposed channel-estimation and equalization algorithms for the EDGE system with time-varying and frequency-selective fading channels, in terms of both estimation mean-square error (MSE) and uncoded BER. The performance

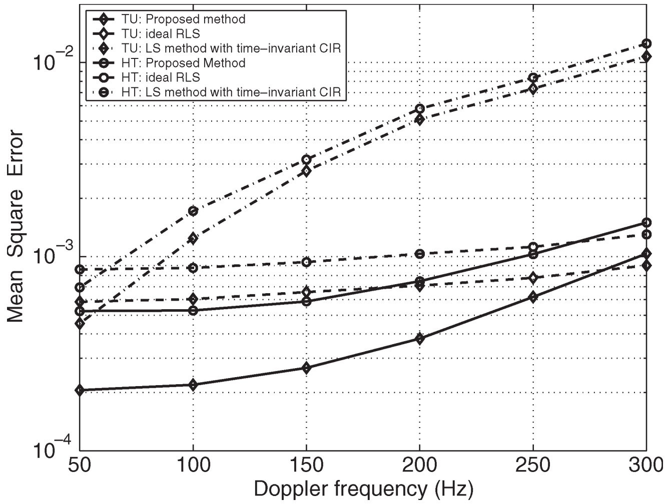

Fig. 5. MSE at frequency range of 50–300 Hz in TU and HT profiles.

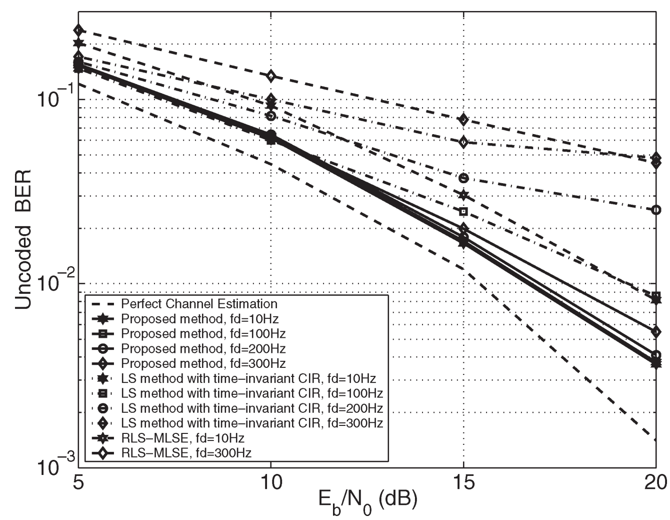

Fig. 6. BER of LS, RLS, and proposed channel-estimation algorithm employing the MLSE equalizer at $f_{\rm d} = 10$, 100, 200, and 300 Hz in TU profile.

is evaluated under the TU and HT channel profiles shown in Fig. 4 [2], and the simulation system is oversampled 37 times to obtain a time resolution of $T_{\rm sample} = T_{\rm sym}/37 \approx 0.1\ \mu$s, which is the minimum differential delay of the multipath branches of the channel. The Rayleigh fading is generated according to [25], and it is independent from burst to burst. The proposed linear interpolated LS-based method estimates the time-varying CIR using the recursive procedure given in (27).

A. MSE

Denote $J_k(l)$ as the MSE of the lth tap CIR at time index k. Assuming we have perfect knowledge of the CIR, the MSE $J_k(l)$ and the time-average MSE $\bar{J}(l)$ can be computed as follows:

$$J_k(l) = E\left([h_k(l) - \hat{h}_k(l)]^\star [h_k(l) - \hat{h}_k(l)]\right) \quad (38)$$

$$\bar{J}(l) = \frac{1}{N_{\rm d}} \sum_{\forall N_{\rm d}} E\left([h_k(l) - \hat{h}_k(l)]^\star [h_k(l) - \hat{h}_k(l)]\right). \quad (39)$$

Fig. 5 depicts the time-average MSE at $E_{\rm b}/N_{\rm o} = 20$ dB computed by various channel-estimation algorithms under different maximum Doppler frequencies in the TU($L = 4$) and HT($L = 7$) profiles. It can be seen from this figure that the proposed estimation algorithm has the smallest time-average MSE when compared to that of the other two algorithms. It is obvious that the Doppler frequency has very little influence on the time-average MSE of the proposed estimation algorithm and the RLS algorithm, while the time-average MSE of the LS algorithm without the channel tracking degrades dramatically with the increase of $f_{\rm d}$. From the figure, it can be concluded that the proposed algorithm can obtain a rather accurate estimation of the time-varying fading channel for a wide range of Doppler frequencies.

Note that the computation of the time-average MSE using the RLS algorithm requires the knowledge of the transmitted symbols, which in practice is unavailable. In Fig. 5, the ideal case of the RLS algorithm, which has a perfect knowledge of the transmitted symbols in the entire burst, is implemented for comparison purposes only. In the next section, the BER performance loss of the RLS algorithm is demonstrated, when the estimated symbols are used for the nonideal channel tracking, which is the practical case.

B. BER Performance

The simulation results for the TU channel profile are depicted in Fig. 6. The BER performance is obtained using various channel-estimation algorithms coupled with the MLSE equalizer. For the perfect channel-estimation case in the figure, it is assumed that the receiver has the perfect knowledge of all the fading channels that are computed using (4). The performance obtained from the perfect channel estimation is shown as a lower bound reference. To enable the adaptive RLS algorithm for the time-varying channel tracking, a joint estimation and equalization is implemented; the RLS estimation algorithm using a step parameter of 0.8 [21] and an MLSE equalizer with a delay output of $2L$. For the TU channel profile, the discrete-time CIR has an effective length of $L = 4$. Hence, the MLSE using the VA with 8^3 states can be employed for a sequence estimation. When the Doppler frequency is low, i.e., $f_{\rm d} = 10$ Hz, the LS and the proposed algorithms have nearly the same BER performance, which is 0.0038 at $E_{\rm b}/N_{\rm o} = 20$ dB. With an increase in Doppler frequency to 100 Hz, the BER performance based on LS algorithm degrades to 0.0087 at the same $E_{\rm b}/N_{\rm o}$. However, the BER performance for the algorithm proposed in this paper still remains the same, and thus, the proposed estimation method has about 2.5-dB gain compared to the LS algorithm. When $f_{\rm d} = 300$ Hz, the CIR may exhibit parabolic behavior, and the BER performance of the LS algorithm degrades dramatically to 0.047 at $E_{\rm b}/N_{\rm o} = 20$ dB. However, there is only a minor loss for the proposed method of this paper. It is obvious that the adaptive RLS algorithm does

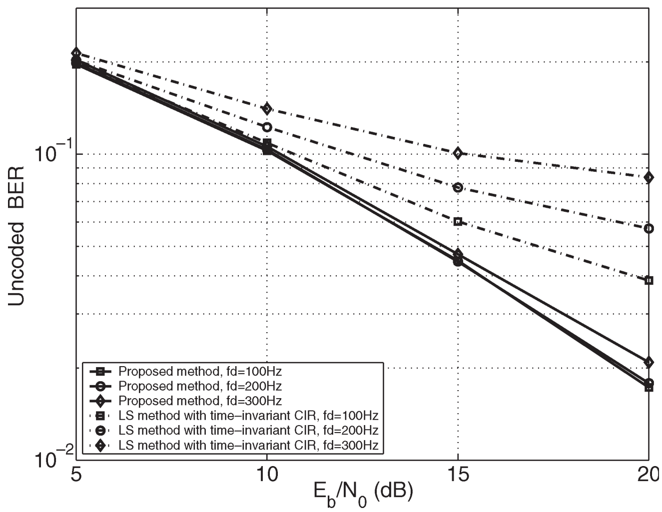

Fig. 7. BER of LS and proposed channel-estimation algorithm employing the DDFSE ($K = 2$) equalizer at $f_{\rm d} = 100$, 200, and 300 Hz in HT profile.

not work very well under the time-varying channel in the EDGE system. The performance loss is mainly due to the delayed output of the MLSE equalizer and the use of the estimated symbols, causing an error propagation in updating the time-varying CIR [3], [23].

Fig. 7 depicts the simulation results using the reduced-state DDFSE equalizer in HT channel profile. The discrete-time CIR with a channel length of $L = 7$ is estimated. For the DDFSE equalizer, only the first $K = 2$ taps of the CIR are used for the trellis diagram with eight states, whereas the remaining taps are fed back for metric calculations. The simulation result shows that the proposed method has a similar BER at Doppler frequencies of 100 and 200 Hz, whereas the LS method has a BER of 0.038 at $E_{\rm b}/N_{\rm o} = 20$ dB and $f_{\rm d} =$ 100 Hz, which presents a loss of about 4 dB compared to the proposed method. From the BER performance, it is evident that the proposed channel-estimation method with Cholesky decomposition, which transforms the estimated discrete-time time-varying CIR into its minimum-phase equivalent form, is a promising method to combat the time-varying channels with low complexity.

VI. Conclusion

In this paper, a linear interpolation LS-based algorithm was presented to estimate the fast time-varying and frequency-selective fading channels of an 8-PSK EDGE system. To enable the use of the reduced-state equalizers, a Cholesky decomposition is performed prior to the equalizer to transform the time-varying CIR into its minimum-phase equivalent form. The proposed algorithm can accurately estimate various fading channels that have a wide range of Doppler frequencies (up to 300 Hz) without the use of the adaptive-tracking algorithms. In terms of the MSE and BER, it was shown via simulations that the proposed algorithm has much better performance than the LS and RLS algorithms, especially for Doppler frequency higher than 100 Hz.

Acknowledgment

The authors would like to thank the anonymous reviewers and the Associate Editor Prof. H. Leib for their helpful comments.

References

[1] S. Nanda, K. Balachandran, and S. Kumar, "Adaptation techniques in wireless packet data services," *IEEE Commun. Mag.*, vol. 38, no. 1, pp. 54–64, Jan. 2000.
[2] ETSI. GSM 05.05, *Radio Transmission and Reception*, Nov. 2000. ETSI EN 300 910 v8.5.1.
[3] W. Gerstacker and R. Schober, "Equalization concepts for EDGE," *IEEE Trans. Wireless Commun.*, vol. 1, no. 1, pp. 190–199, Jan. 2002.
[4] J. C. Olivier, S. Y. Leong, C. Xiao, and K. D. Mann, "Efficient equalization and symbol detection for 8-PSK EDGE cellular system," *IEEE Trans. Veh. Technol.*, vol. 52, no. 3, pp. 525–529, May 2003.
[5] A. Duel-Hallen and C. Heegard, "Delayed decision-feedback sequence estimation," *IEEE Trans. Commun.*, vol. 37, no. 5, pp. 428–436, May 1989.
[6] M. V. Eyuboglu and S. U. Qureshi, "Reduced-state sequence estimation with set partitioning and decision feedback," *IEEE Trans. Commun.*, vol. 36, no. 1, pp. 13–20, Jan. 1988.
[7] C. F. N. Cowan and P. M. Grant, *Adaptive Filters*. Englewood Cliffs, NJ: Prentice-Hall, 1985.
[8] N. Zhou and N. Holte, "Least squares channel estimation for a channel with fast time variation," in *Proc. IEEE ICASSP*, Mar. 1992, vol. 5, pp. 165–168.
[9] J. Chen and Y. Wang, "Adaptive MLSE equalizers with parametric tracking for multipath fast fading channels," *IEEE Trans. Commun.*, vol. 49, no. 4, pp. 655–663, Apr. 2001.
[10] M. Schmidt and G. P. Fettweis, "FIR prefiltering for near optimum phase target channels," in *Proc. 6th Can. Workshop Inf. Theory*, Jun. 1999.
[11] B. Yang, "An improved fast algorithm for computing the MMSE decision-feedback equalizer," *Int. J. Electron. Commun.*, vol. 53, no. 1, pp. 1–6, 1999.
[12] N. Al-Dhahir and J. M. Cioffi, "MMSE decision-feedback equalizers: Finite-length results," *IEEE Trans. Inf. Theory*, vol. 41, no. 4, pp. 961–975, Jul. 1995.
[13] ——, "Fast computation of channel-estimate based equalizers in packet data transmission," *IEEE Trans. Signal Process.*, vol. 43, no. 11, pp. 2462–2473, Jul. 1995.
[14] W. H. Gerstacker, F. Obernorsterer, R. Meyer, and J. B. Huber, "An efficient method for prefilter computation for reduced-state equalization," in *Proc. IEEE Int. Symp. Pers., Indoor, Mobile RadioCommun.*, London, U.K., Sep. 2000, pp. 604–609.
[15] K. Chang and C. N. Georghiades, "Iterative joint sequence and channel estimation for fast time-varying intersymbol interference channels," in *Proc. IEEE ICC 95*, Jun. 1995, vol. 1, pp. 357–361.
[16] C. Xiao, J. Wu, S.-Y. Leong, Y. R. Zheng, and K. B. Letaief, "A discrete-time model for triply selective MIMO Rayleigh fading channels," *IEEE Trans. Wireless Commun.*, vol. 3, no. 5, pp. 1678–1688, Sep. 2004.
[17] P. Jung, "Laurent's representation of binary digital continuous phase modulated signals with modulation index 1/2 revisited," *IEEE Trans. Commun.*, vol. 42, no. 234, pp. 221–224, Apr. 1994.
[18] H. Olofsson and A. Furuskar, "Aspects of introducing EDGE in existing GSM networks," in *Proc. IEEE Int. Conf. Universal Pers. Commun.*, 1998, vol. 1, pp. 421–426.
[19] J. G. Proakis, *Digital Communications*, 4th ed. New York: McGraw-Hill, 2001, pp. 623–624.
[20] G. L. Stuber, *Principle of Mobile Communication*, 2nd ed. Norwell, MA: Kluwer, 2001.
[21] S. Haykin, *Adaptive Filter Theory*, 3rd ed. Englewood Cliffs, NJ: Prentice-Hall, 1996.
[22] J. C. Olivier and C. Xiao, "Joint optimization of FIR prefilter and channel estimate for sequence estimation," *IEEE Trans. Commun.*, vol. 50, no. 9, pp. 1401–1404, Sep. 2002.
[23] K. A. Hamied and G. L. Stuber, "An adaptive truncated MLSE receiver for Japanese personal digital cellular," *IEEE Trans. Veh. Technol.*, vol. 45, no. 1, pp. 41–50, Feb. 1996.
[24] A. Klein, G. K. Kaleh, and P. W. Baier, "Zero forcing and minimum mean-square-error equalization for multiuser detection in code-division multiple-access channels," *IEEE Trans. Veh. Technol.*, vol. 45, no. 2, pp. 276–287, May 1996.

[25] Y. R. Zheng and C. Xiao, "Improved models for the generation of multiple uncorrelated Rayleigh fading waveforms," *IEEE Commun. Lett.*, vol. 6, no. 6, pp. 256–258, Jun. 2002.

Sang-Yick Leong received the B.S., M.S.(EE), and Ph.D. degrees from the University of Missouri-Columbia, Columbia, in 1999, 2001, and 2005, respectively.

His research interests include the physical layer of wireless communications, which include MIMO channel modeling, capacity of MIMO mobile-radio channels, space-time coding, channel estimation and equalization, and spread spectrum communications.

Jingxian Wu received the B.S.(EE) degree from the Beijing University of Aeronautics and Astronautics, Beijing, China, in 1998, the M.S.(EE) degree from Tsinghua University, Beijing, China, in 2001 and the Ph.D. degree from the University of Missouri at Columbia, in 2005.

He is an Assistant Professor with the Department of Engineering Science, Sonoma State University, Rohnert Park, CA. His research interests include the physical layer of wireless communication systems, including error performance analysis, space-time coding, channel estimation and equalization, and spread spectrum communications.

Dr. Wu is a member of Tau Beta Pi.

Chengshan Xiao (M'99–SM'02) received the B.S. degree from the University of Electronic Science and Technology of China, Chengdu, China, in 1987, the M.S. degree from Tsinghua University, Beijing, China, in 1989 and the Ph.D. degree from the University of Sydney, Sydney, Australia, in 1997, all in electrical engineering.

From 1989 to 1993, he was on the Research Staff and then became a Lecturer with the Department of Electronic Engineering at Tsinghua University. From 1997 to 1999, he was a Senior Member of the Scientific Staff with Nortel Networks, Ottawa, ON, Canada. From 1999 to 2000, he was an Assistant Professor with the Department of Electrical and Computer Engineering at the University of Alberta, Edmonton, AB, Canada. He is currently a Faculty Member with the Department of Electrical and Computer Engineering at the University of Missouri, Columbia. His research interests include wireless communication networks, signal processing, and multidimensional and multirate systems. He has published extensively in these areas. He holds three United States patents in wireless communications. His algorithms have been implemented into Nortel's base-station radios with successful technical field trials and network integrations.

Dr. Xiao has been an Editor for the IEEE TRANSACTIONS ON WIRELESS COMMUNICATIONS since July 2002. Previously, he was an Associate Editor for the IEEE TRANSACTIONS ON VEHICULAR TECHNOLOGY, the IEEE TRANSACTIONS ON CIRCUITS AND SYSTEMS—I, and the international journal *Multidimensional Systems and Signal Processing*. He has been involved in organizing major international conferences. These include serving as Technical Program Chair for the 2007 IEEE Wireless Communications and Networking Conference and Vice Chair for the 2005 IEEE Globecom Wireless Communications Symposium. He has also served as a Technical Program Committee member for a number of IEEE international conferences including ICC, Globecom, and WCNC in the last few years. He is currently the Vice Chair of the IEEE Communications Society Technical Committee on Personal Communications.

Jan C. Olivier received the B.Eng., M.Eng., and Ph.D. degrees (*summa cum laude*) from the University of Pretoria, Pretoria, South Africa, in 1985, 1986, and 1990, respectively.

He was with the National Institute for Defense Research, Pretoria, until 1992 and then with Potchefstroom University and the University of Pretoria as an Associate Professor until 1995. He was a Member of the Scientific Staff with Bell Northern Research (BNR) Ottawa, ON, Canada, until 1999 and a Principle Scientist with the Nokia Research Laboratory in Texas until July 2003, when he joined the University of Pretoria as a Professor. His research interests include estimation, detection, inference, and numerical methods.